Asian Journal of Chemistry; Vol. 38, No. 9 (2026), 2510-2518
ASIAN JOURNAL OF CHEMISTRY
https://doi.org/10.14233/ajchem.2026.36415

Triazine-Sulfonamide Hybrids: Synthesis, Antimicrobial Evaluation and *In silico* Investigation of their Potential Interaction with Dihydrofolate Reductase (DHFR)

NISHAM RANI[1], MOHIT MANGLA[1,*], MOHIT SANDUJA[2,*] and MEGHA[3]

[1]School of Healthcare and Allied Sciences, GD Goenka University, Sohna-122103, India
[2]School of Pharmacy and Research, Dev Bhoomi Uttarakhand University, Dehradun-248001, India
[3]Department of Chemistry, Centre of Advanced Study, Guru Nanak Dev University, Amritsar-143005, India

*Corresponding author: E-mail: mohitpharmacist@gmail.com; drmohitsanduja@gmail.com

Received: 13 May 2026 *Accepted*: 28 August 2026 *Published online*: 5 September 2026 AJC-22480

Triazine–sulfonamide hybrids offer a versatile scaffold for antimicrobial drug, with the triazine core enabling structural modification and the sulfonamide group supporting target interactions. DHFR inhibition by these hybrids provides a rational strategy for developing new antimicrobial agents against the growing challenge of AMR. Hence, the present study focuses on the synthesis, structural characterization and evaluation of triazine–sulfonamide hybrids (**A$_1$–A$_{12}$**) for DHFR binding, supported by integrated *in silico* modelling and *in vitro* antimicrobial studies. Molecular docking with DHFR (PDB ID: 1RX3) showed good binding affinities (-8.5 to -10.2 kcal/mol), with key hydrogen-bonding interactions involving Asp27, Arg52, Arg57 and Ile94. Compounds **A$_1$** and **A$_{12}$** showed stronger binding than ciprofloxacin (-9.1 kcal/mol) and trimethoprim (-7.6 kcal/mol), which support its potential as DHFR-targeting antimicrobial candidates. *In vitro* antimicrobial screening *via* the tube dilution method demonstrated broad-spectrum potency across bacterial and fungal strains: compound **A$_1$** exhibited the lowest MIC against *Escherichia coli* (1.05 ± 0.06 μg/mL), compound **A$_{10}$** against *Staphylococcus aureus* (2.11 ± 0.08 μg/mL), compound **A$_4$** against *Bacillus subtilis* (2.14 ± 0.08 μg/mL) and *Candida albicans* (1.11 ± 0.05 μg/mL), compound **A$_{12}$** against *Pseudomonas aeruginosa* (1.19 ± 0.05 μg/mL) and compound **A$_5$** against *Aspergillus niger* (2.41 ± 0.09 μg/mL). Molecular dynamics (MD) simulations confirmed the dynamic stability and structural integrity of the top performing ligand DHFR complexes under simulated physiological conditions. DFT calculations provided insight into the frontier molecular orbitals and chemical reactivity descriptors, supporting the electronic stability and reactivity of the active scaffolds.

Keywords: Triazine, Sulfonamide, Molecular simulations, Antimicrobial resistance, DHFR.

INTRODUCTION

Triazine–sulfonamide hybrids represent an attractive scaffold for antimicrobial drug discovery through the combination of two pharmacophoric motifs within a single molecular framework. The electron-deficient 1,3,5-triazine nucleus undergoes versatile nucleophilic substitution, enabling structural diversification and systematic structure–activity relationship (SAR) studies [1,2]. Triazine derivatives, particularly diamino triazines, have shown activity against bacterial dihydrofolate reductase (DHFR), supporting their potential as antifolate scaffolds [3-6].

Sulfonamides are established pharmacophores in anti-infective drug development and continue to attract interest as antibacterial agents [7-12]. Incorporation of the sulfonamide group into hybrid structures can influence hydrogen bonding, electronic characteristics, lipophilicity and molecular recognition. Sulfonamide containing conjugates have reported antibacterial activity together with DHFR inhibition, supporting their combination with scaffolds capable of interacting with folate-pathway targets [13-17].

DHFR is an established antimicrobial target that catalyzes the NADPH-dependent reduction of dihydrofolate to tetrahydrofolate, maintaining the reduced folate pool required for one-carbon transfer reactions and nucleotide biosynthesis [18-22]. Inhibition of microbial DHFR disrupts folate metabolism and restricts bacterial growth. The availability of structurally characterized DHFR–inhibitor complexes has further supported structure-based development of new antimicrobial agents [23-25]. Trimethoprim provides clinical validation of bacterial DHFR as an antibacterial target, while the emergence of resistance has increased the need for structurally diverse DHFR inhibitors [26,27].

Substituted 1,3,5-triazine-2,4-diamines have been reported to bind and inhibit bacterial DHFR, with some derivatives exhibiting nanomolar enzyme inhibition. Molecular docking and kinetic studies have supported their binding within the dihydrofolate-binding region, providing a basis for further structural optimization [28,29]. Despite this progress, systematic studies on triazine–sulfonamide hybrids as DHFR-directed antimicrobial agents remain limited, particularly those integrating synthesis, molecular modelling, enzyme inhibition and whole-cell antimicrobial evaluation. The present study addersses this gap through the synthesis of triazine–sulfonamide hybrids followed by structural characterization and *in silico* and *in vitro* evaluation. Molecular docking was employed to examine DHFR binding modes and ligand–target interactions, while antimicrobial and DHFR inhibitory assays were used to assess biological activity.

EXPERIMENTAL

All starting materials used were of analytical grade and procured from various sources, including Loba Chem Pvt. Ltd. and HI Media Pvt Ltd. (New Delhi, India). Thin-layer chromatography (TLC) was performed using silica gel G as the stationary phase and a mixture of ethyl acetate and *n*-hexane as the mobile phase. Melting points were determined using a sonar melting point instrument (Sunbim, India) and are uncorrected. ^{1}H NMR spectra were recorded using a TopSpin 3.2 400 MHz NMR spectrometer (Bruker Corporation, India) with DMSO as the solvent. Mass spectra were recorded using a Micromass Q-ToF Micro instrument. A laminar airflow biosafety cabinet (Hisar, India) and a BOD incubator (Laborate Pharmaceutical India Ltd., India) were used for determining minimum inhibitory concentrations (MIC). Molecular docking studies were performed using GROMACS (New York, USA), while chemical structures were drawn using ChemDraw Professional 15.0 (USA).

Synthesis: In the first step, cyanuric chloride was subjected to nucleophilic substitution with sulfanilamide. Sulfanilamide (1 equiv.) was added gradually over 2 min to an ice-cooled, magnetically stirred solution of cyanuric chloride in dry acetone. The reaction mixture was stirred at 0-5 ºC until complete consumption of the starting materials, as confirmed by TLC (*n*-hexane/acetone, 2:3). The HCl generated during the reaction was neutralized by the gradual addition of $NaHCO_3$ solution (1 equiv.), followed by stirring for 10 min. Crushed ice (100 mL) was then added and the precipitated product was collected by suction filtration and dried under vacuum overnight at 30-40 ºC. In the next step, *N*′-(4,6-dichloro-1,3,5-triazin-2-yl)benzenesulfonamide (0.01 mol) was dissolved in acetone (15 mL) and treated with substituted anilines (0.01 mol). A 4% NaOH solution was added dropwise at room temperature and the reaction mixture was stirred for 3 h. The mixture was poured onto crushed ice with constant stirring and neutralized with dilute HCl. The resulting solid was filtered, washed with water, dried and recrystallized. Finally, this product (0.01 mol) dissolved in DMF (15 mL) was treated with substituted amines (0.01 mol). A 4% K_2CO_3 solution was added dropwise at room temperature and the reaction mixture was stirred for 1 h. The mixture was then poured onto crushed ice with constant stirring and neutralized with dilute HCl. The resulting solid (**A_1–A_{12}**) was filtered, washed with water, dried and recrystallized (**Scheme-I**).

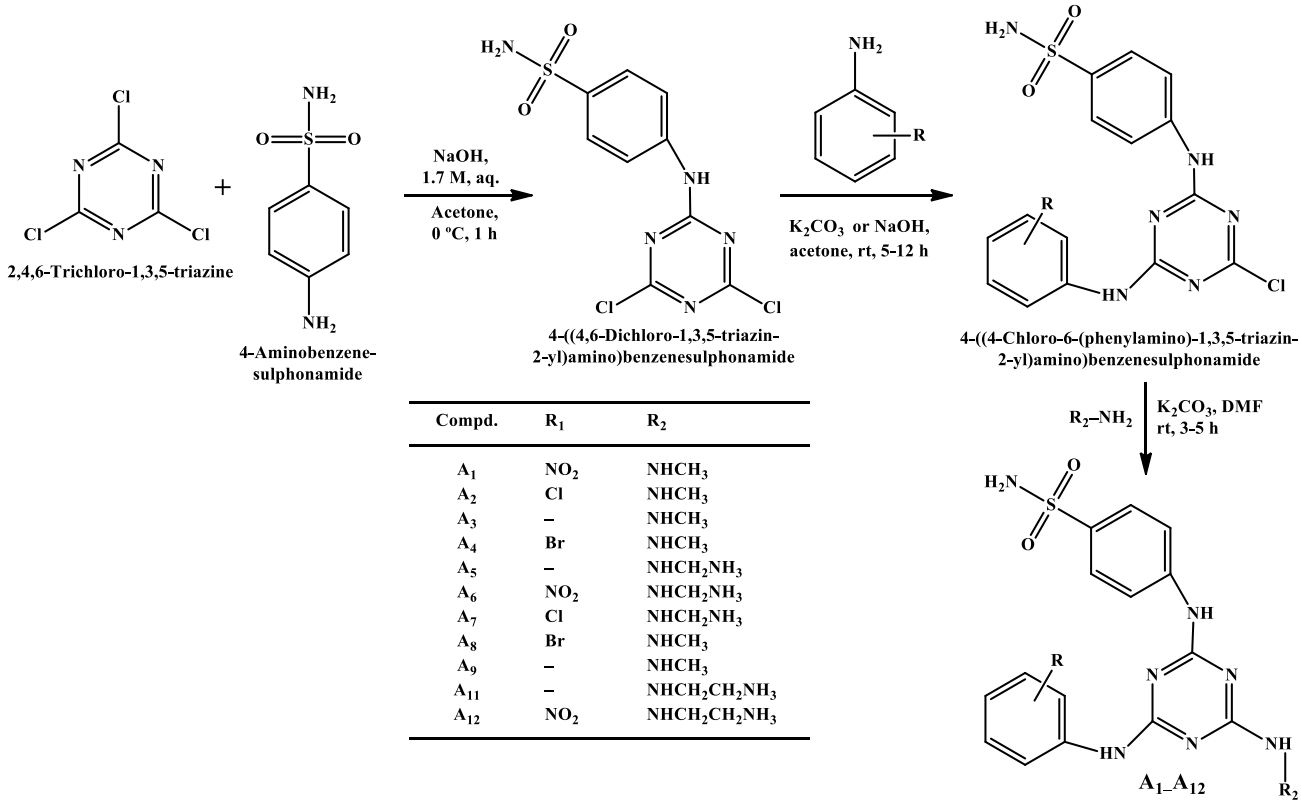

Compd.	R_1	R_2
A_1	NO_2	$NHCH_3$
A_2	Cl	$NHCH_3$
A_3	–	$NHCH_3$
A_4	Br	$NHCH_3$
A_5	–	$NHCH_2NH_3$
A_6	NO_2	$NHCH_2NH_3$
A_7	Cl	$NHCH_2NH_3$
A_8	Br	$NHCH_3$
A_9	–	$NHCH_3$
A_{11}	–	$NHCH_2CH_2NH_3$
A_{12}	NO_2	$NHCH_2CH_2NH_3$

Scheme-I: Synthetic route for the synthesis of triazine-sulphonamide derivatives

4-((4-(*tert*-Butylamine)-6-((4-nitrophenyl)amino)-1,3,5-triazin-2-yl)amino)benzene sulfonamide (A_1): Yield: 36%, m.p.: 210-212 ºC, R_f: 0.31, m.f.: $C_{19}H_{22}N_8O_4S$ (*m.w.*: 432.93 g/mol); MS: 459.5 (M^{+1}); IR (KBr, ν_{max}, cm^{-1}): 3375 (N–H *str.*), 3100 (C–H *str.*, Ar.), 2984 (C–H *str.*, aliph.), 1650 (C=N *str.*, triazine), (NO_2 asym. *str.*), 1360 (NO_2 sym. *str.*), 1350 and 1150 (SO_2 *str.*), 825 (C–S *str.*); ^{1}H NMR (500 MHz, DMSO-d_6, δ ppm): 9.02 (s, 1H), 8.83 (s, 1H), 8.22 (d, *J* = 8.8 Hz, 2H), 7.91 (d, *J* = 8.8 Hz, 2H), 7.74 (d, *J* = 8.5 Hz, 2H), 7.42 (d, *J* = 8.5 Hz, 2H), 7.18 (s, 2H), 6.82 (s, 1H), 1.29 (s, 9H). ^{13}C NMR (125 MHz, DMSO-d_6, δ ppm): 167.3, 165.8, 163.9, 146.5, 143.8, 141.7, 137.2, 129.8, 127.4, 125.6, 123.8, 119.5, 50.8, 29.4.

4-((4-((4-Chlorophenyl)amino-6-(methylamino)-1,3,5-triazine-2-yl)amino)benzene sulfonamide (A_2): Yield: 45%, m.p.: 243-245 ºC, R_f: 0.41, m.f.: $C_{17}H_{17}ClN_7O_2S$ (*m.w.*: 432.93 g/mol); MS: 406.86 (M^{+1}); IR (KBr, ν_{max}, cm^{-1}): 3300 (N–H *str.*), 3100 (C–H *str.*, Ar.), 2984 (C–H *str.*, aliph.), 1650 (C=N *str.*, 1,3,5-triazine), 1350 (SO_2 asym. *str.*), 1135 (SO_2 sym. *str.*), 825 (C–S *str.*), 680 (C–Cl *str.*); ^{1}H NMR (500 MHz, DMSO-d_6, δ ppm): 9.08 (s, 1H), 8.76 (s, 1H), 7.82 (d, *J* = 8.7 Hz, 2H, Ar–H), 7.56 (d, *J* = 8.7 Hz, 2H), 7.41 (d, *J* = 8.6 Hz, 2H), 7.22 (d, *J* = 8.6 Hz, 2H), 7.10 (s, 2H), 6.95 (s, 1H), 2.88 (d, *J* = 4.8 Hz); ^{13}C NMR (125 MHz, DMSO-d_6, δ ppm): 166.8, 165.4, 163.7, 145.8, 139.6, 136.2, 133.5, 129.6, 128.9, 127.5, 125.8, 122.4, 118.7, 28.7.

4-((4-(Methylamino)-6-(phenylamino)1,3,5-triazine-2-yl)amino)benzene sulfonamide (A_3): Yield: 40%, m.p.: 213-215 ºC, R_f: 0.38, m.f.: $C_{17}H_{18}N_7O_2S$ (*m.w.*: 371.42 g/mol); MS: 373.13 (M^{+1}); IR (KBr, ν_{max}, cm^{-1}): 3375 (N–H *str.*), 3100 (C–H *str.*, Ar.), 2980 (C–H *str.*, aliph.), 1650 (C=N *str.*, 1,3,5-triazine), 1350 (SO_2 asym. *str.*), 1186 (SO_2 sym. *str.*), 850-670 (C–S *str.*); ^{1}H NMR (500 MHz, DMSO-d_6, δ ppm): 9.04 (s, 1H), 8.71 (s, 1H), 7.76 (d, *J* = 8.6 Hz, 2H), 7.49 (d, *J* = 8.6 Hz, 2H), 7.36-7.31 (m, 2H), 7.17-7.12 (m, 2H), 6.98-6.93 (m, 1H), 7.08 (s, 2H), 6.87 (s, 1H), 2.86 (d, *J* = 4.9 Hz, 3H); ^{13}C NMR (125 MHz, DMSO-d_6, δ ppm): 166.7, 165.2, 163.8, 145.4, 139.5, 138.2, 129.5, 128.8, 127.3, 124.6, 122.1, 119.3, 28.6.

4-((4-(Bromophenyl)amino)-6-(methylamino)1,3,5-triazine-2-yl)amino)benesulfonamide (A_4): Yield: 42%, m.p.: 232-234 ºC, R_f: 0.28, m.f.: $C_{17}H_{17}BrN_7O_2S$ (*m.w.*: 450.31 g/mol); MS: 451.03 (M^{+1}); IR (KBr, ν_{max}, cm^{-1}): 3300 (N–H *str.*), 3100 (C–H *str.*, Ar.), 2984 (C–H *str.*, aliph.), 1650 (C=N *str.*), 1350 (SO_2 asym. *str.*), 1180 (SO_2 sym. *str.*), 750 (C–S *str.*), 650 (C–Br *str.*); ^{1}H NMR (500 MHz, DMSO-d_6, δ ppm): 9.06 (s, 1H), 8.74 (br s, 1H), 7.79 (d, *J* = 8.6 Hz, 2H), 7.61 (d, *J* = 8.5 Hz, 2H), 7.52 (d, *J* = 8.7 Hz, 2H), 7.29 (d, *J* = 8.7 Hz, 2H), 7.11 (br s, 2H), 6.91 (br s, 1H), 2.87 (d, *J* = 4.8 Hz, 3H); ^{13}C NMR (125 MHz, DMSO-d_6, δ ppm): 166.9, 165.5, 163.8, 145.7, 139.7, 137.4, 132.1, 129.8, 128.9, 127.6, 123.5, 122.3, 119.1, 28.8.

4-((4-Ethylamino)-6-(4*H*-1,4-oxazin-4yl)-1,3,5-triazine-2-yl)amino)benzene sulfonamide (A_5): Yield: 39%, m.p.: 243-245 ºC, R_f: 0.31, m.f.: $C_{17}H_{22}N_8O_3S$ (*m.w.*: 375.41 g/mol); MS: 392.15 (M^{+1}); IR (KBr, ν_{max}, cm^{-1}): 3300 (N–H *str.*), 3100 (C–H *str.*), 2980 (C–H *str.*, aliph.), 1650 (C=N *str.*), 1350 (SO_2 *str.*), 1180 (SO_2 *str.*), 1050 (C–O–C), 650 (C–S *str.*); ^{1}H NMR (500 MHz, DMSO-d_6, δ ppm): 9.22 (s, 1H), 7.84-7.78 (m, 4H), 7.72 (d, *J* = 8.6 Hz, 2H), 7.23 (d, *J* = 8.6 Hz, 2H), 4.07 (t, *J* = 5.2 Hz, 4H), 3.57 (t, *J* = 5.2 Hz, 4H), 3.28 (q, *J* = 7.2 Hz, 2H), 1.13 (t, *J* = 7.2 Hz, 3H); ^{13}C NMR (125 MHz, DMSO-d_6, δ ppm): 166.85, 165.72, 163.58, 144.21, 141.63, 136.89, 128.42, 123.96, 118.37, 67.18, 49.84, 37.91, 14.63.

4-((4-Ethylamino)-6-(4*H*-1,4-oxazin-4yl)-1,3,5-triazine-2-yl)amino)benzene sulfonamide (A_6): Yield: 40%, m.p.: 209-211 ºC, R_f: 0.41, m.f.: $C_{17}H_{22}N_8O_3S$ (*m.w.*: 430.44 g/mol); MS: 392.42 (M^{+1}); IR (KBr, ν_{max}, cm^{-1}): 3300 (N–H *str.*), 3100 (C–H *str.*, Ar.), 2984 (C–H *str.*, aliph.), 1650 (C=N *str.*, 1,3,5-triazine), 1350 (SO_2 asym. *str.*), 1180 (SO_2 sym. *str.*), 1050 (C–O–C *str.*, oxazine), 750 (C–S *str.*); ^{1}H NMR (500 MHz, DMSO-d_6, δ ppm): 9.21 (s, 1H), 7.83-7.76 (m, 3H), 7.72 (d, *J* = 8.6 Hz, 2H), 7.22 (d, *J* = 8.6 Hz, 2H), 4.06 (t, *J* = 5.2 Hz, 4H), 3.56 (t, *J* = 5.2 Hz, 4H), 3.27 (q, *J* = 7.1 Hz, 2H), 1.12 (t, *J* = 7.1 Hz, 3H); ^{13}C NMR (125 MHz, DMSO-d_6, δ ppm): 167.38, 166.12, 164.79, 144.56, 140.82, 136.74, 128.55, 123.42, 118.64, 66.98, 49.52, 38.15, 14.76.

4-((4-((4-Chlorophenylamino)-6-(propylamino)-1,3,5-triazine-2-yl)amino)benzene sulfonamide (A_7): Yield: 41%, m.p.: 256-258 ºC, R_f: 0.43, m.f.: $C_{19}H_{22}ClN_7O_2S$ (*m.w.*: 419.89 g/mol); MS: 421.91 (M^{+}); IR (KBr, ν_{max}, cm^{-1}): 3300 (N–H *str.*), 3100 (C–H *str.*, Ar.), 2984 (C–H *str.*, aliph.), 1650 (C=N *str.*, 1,3,5-triazine), 1350 (SO_2 asym. *str.*), 1150 (SO_2 sym. *str.*), 750 (C–S *str.*), 650 (C–Cl *str.*); ^{1}H NMR (500 MHz, DMSO-d_6, δ ppm): 9.34 (s, 1H), 8.82 (s, 1H), 7.84-7.77 (m, 4H), 7.55 (d, *J* = 8.7 Hz, 2H), 7.38 (d, *J* = 8.6 Hz, 2H), 7.22 (d, *J* = 8.6 Hz, 2H), 6.98 (d, *J* = 8.7 Hz, 2H), 3.18 (q, *J* = 6.8 Hz, 2H), 1.54–1.47 (m, 2H), 0.89 (t, *J* = 7.4 Hz, 3H); ^{13}C NMR (125 MHz, DMSO-d_6, δ ppm): 167.82, 166.45, 164.94, 144.38, 141.26, 137.82, 135.46, 129.31, 128.54, 124.37, 122.61, 118.83, 115.72, 42.63, 22.51, 11.63.

4-((4-((4-Bromophenyl)amino)-6-(ethylamino)-1,3,5-triazin-2-yl)amino)benzene sulfonamide (A_8): Yield: 54%, m.p.: 222-224 ºC, R_f: 0.34, m.f.: $C_{18}H_{20}BrN_7O_2S$ (*m.w.*: 464.34 g/mol); MS: 452 (M^{+2}); IR (KBr, ν_{max}, cm^{-1}): 3300 (N–H *str.*), 3100 (C–H *str.*, Ar.), 2984 (C–H *str.*, aliph.), 1650 (C=N *str.*, 1,3,5-triazine), 1350 (SO_2 asym. *str.*), 1150 (SO_2 sym. *str.*), 750 (C–S *str.*), 550 (C–Br *str.*); ^{1}H NMR (500 MHz, DMSO-d_6, δ ppm): 8.97 (s, 1H), 8.85-8.80 (m, 1H), 7.94-7.88 (m, 1H), 7.86-7.80 (m, 1H), 7.74-7.68 (m, 1H). ^{13}C NMR (125 MHz, $CDCl_3$, δ ppm): 168.71, 168.66, 162.93, 152.13, 152.10, 152.09, 152.07, 152.03, 152.00, 136.68, 136.67, 136.61, 136.60, 135.06, 135.01, 131.71, 131.70, 131.69, 130.59, 130.56, 130.53, 130.51, 124.57, 124.56, 124.52, 124.50, 122.29, 122.23.

4-((4-(Ethylamino)-6-(phenylamino)-1,3,5-triazin-2-yl)amino)benzene sulfonamide (A_9): Yield: 37%, m.p.: 230-222 ºC, R_f: 0.39, m.f.: $C_{18}H_{20}N_7O_2S$ (*m.w.*: 353.42 g/mol); MS: 388.15 (M^{+1}); IR (KBr, ν_{max}, cm^{-1}): 3300 (N–H *str.*), 3100 (C–H *str.*, Ar.), 2984 (C–H *str.*, aliph.), 1650 (C=N *str.*), 1350 (SO_2 asym. *str.*), 1150 (SO_2 sym. *str.*), 750 (C–S *str.*). ^{1}H NMR (500 MHz, DMSO-d_6, δ ppm): 9.82 (s, 1H), 9.18 (s, 1H), 8.05 (br s, 2H), 7.62 (d, 2H), 7.38 (d, 2H), 7.31-7.25 (m, 2H), 7.08-7.03 (m, 2H), 6.92-6.88 (m, 1H), 7.48 (s, 1H), 3.32 (q, 2H), 1.12 (t, 3H); ^{13}C NMR (125 MHz, DMSO-d_6, δ ppm): 168.8, 167.2, 165.4, 145.2, 139.6, 129.5, 128.8, 127.3, 124.9, 121.8, 118.6, 114.9, 36.4, 15.1.

4-((4-(4*H*-1,4-Oxazin-4-yl)-6-(propylamino)-1,3,5-triazine-2-yl)amino)benzene sulfonamide (A10): Yield: 42%, m.p.: 229-231 ºC, R_f: 0.48, m.f.: $C_{18}H_{23}N_7O_3S$ (*m.w.*: 389.43 g/mol); MS: 392.15 (M^{+1}); IR (KBr, ν_{max}, cm^{-1}): 3300 (N–H *str.*), 3100 (C–H *str.*, Ar.), 2984 (C–H *str.*, aliph.), 1650 (C=N *str.*, 1,3,5-triazine), 1350 (SO_2 asym. *str.*), 1150 (SO_2 sym. *str.*), 1050 (C–O–C *str.*, oxazine), 750 (C–S *str.*); ^{1}H NMR (500 MHz, DMSO-d_6, δ ppm): 9.25 (s, 1H), 8.02 (s, 2H, SO_2NH_2), 7.60 (d, 2H), 7.35 (d, 2H), 7.46 (s, 1H), 3.82-3.76 (m, 4H), 3.62-3.56 (m, 4H), 3.18 (q, 2H), 1.52-1.45 (m, 2H), 0.90 (t, 3H); ^{13}C NMR (125 MHz, DMSO-d_6, δ ppm): 168.9, 166.8, 165.1, 145.4, 128.9, 126.7, 118.2, 114.8, 66.4, 49.6, 41.3, 22.6, 11.8.

4-((4-((4-Chlorophenyl)amino)-6-(propylamino)-1,3,5-triazine-2-yl)amino)benzenesulfonamide (A11): Yield: 54%, m.p.: 223-225 ºC, R_f: 0.40, m.f.: $C_{19}H_{22}ClN_7O_2S$ (*m.w.*: 433.92 g/mol); MS: 423 (M^{+2}); IR (KBr, ν_{max}, cm^{-1}): 3300 (N–H *str.*), 3100 (C–H *str.*, Ar.), 2984 (C–H *str.*, aliph.), 1650 (C=N *str.*), 1350 (SO_2 asym. *str.*), 1150 (SO_2 sym. *str.*), 750 (C–S *str.*), 650 (C–Cl *str.*); ^{1}H NMR (500 MHz, DMSO-d_6, δ ppm): 9.85 (s, 1H), 9.18 (s, 1H), 8.03 (br s, 2H), 7.63 (d, 2H), 7.41 (d, 2H), 7.36 (d, 2H), 7.12 (d, 2H), 7.50 (s, 1H), 3.18 (q, 2H), 1.55-1.47 (m, 2H), 0.91 (t, 3H); ^{13}C NMR (125 MHz, DMSO-d_6, δ ppm): 168.9, 167.4, 165.3, 145.1, 138.6, 130.8, 129.6, 128.8, 127.2, 124.9, 121.6, 116.0, 41.0, 22.5, 11.0.

4-((4-((4-Nitrophenyl)amino)-6-(propylamino)-1,3,5-triazin-2-yl)amino)benzene sulfonamide (A12): Yield: 51%, m.p.: 241-243 ºC, R_f: 0.58, m.f.: $C_{19}H_{22}N_8O_4S$ (*m.w.*: 433.11 g/mol); MS: 433.47 (M^{+1}); IR (KBr, ν_{max}, cm^{-1}): 3300 (N–H *str.*), 3100 (C–H *str.*, Ar.), 2984 (C–H *str.*, aliph.), 1650 (C=N *str.*, 1,3,5-triazine), 1520 (NO_2 asym. *str.*), 1350 (NO_2 sym. *str.*), 1300 (SO_2 asym. *str.*), 1150 (SO_2 sym. *str.*), 750 (C–S *str.*); ^{1}H NMR (500 MHz, DMSO-d_6, δ ppm): 10.12 (s, 1H), 9.24 (s, 1H), 8.08 (s, 2H), 8.18 (d, 2H), 7.63 (d, 2H), 7.48 (d, 2H), 7.40 (d, 2H), 7.52 (br s, 1H), 3.19 (q, 2H), 1.54-1.47 (m, 2H), 0.91 (t, 3H); ^{13}C NMR (125 MHz, DMSO-d_6, δ ppm): 169.1, 167.6, 165.4, 147.8, 145.3, 141.6, 129.4, 128.8, 125.3, 124.6, 121.7, 116.0, 41.3, 22.5, 11.7.

Molecular docking analysis: Molecular docking was performed using the AutoDock against the dihydrofolate reductase (PDB ID: 1RX3). The protein was prepared using the protein preparation wizard (hydrogen addition, bond order assignment, PROPKA pH 7.4, OPLS4 energy minimization, RMSD 0.30 Å). Ligands were prepared using LigPrep/Epik at pH 7.4 ± 2.0. A receptor grid box of 20 Å × 20 Å × 20 Å was placed around the substrate-binding channel, with Ile94, Asp27, Arg52 and Arg57 located within the docking region. Optimal poses were selected based on GScore and interaction analysis and binding free energies were estimated using MM-GBSA. Ciprofloxacin was used as the reference standard.

Antimicrobial activity: The synthesized compounds (**A1–A12**) were evaluated for *in vitro* antimicrobial activity by the standard tube dilution method and their minimum inhibitory concentrations (MICs) were determined. The compounds were tested against Gram-positive bacteria *S. aureus* (MTCC 3160) and *B. subtilis* (MTCC 441), Gram-negative *P. aeruginosa* (MTCC 2488) and *E. coli* (MTCC 443) and fungi *C. albicans* (MTCC 227) and *A. niger* (MTCC 281), using ciprofloxacin as the reference drug. Serial dilutions of the test compounds and standard were prepared in double-strength nutrient broth for bacterial strains and Sabouraud dextrose broth for fungal strains. The cultures were incubated at 37 ± 1 ºC for 24 h (bacteria), 37 ± 1 ºC for 48 h (*C. albicans*) and 25 ± 1 °C for 7 days (*A. niger*).

Molecular dynamic (MD) simulation: The software GROMACS 2022.2 was used to conduct molecular dynamics (MD) simulations, Ligands **A1**, **A12** and standard drug ciprofloxacin were selected based on their docking score, binding interactions and pharmacokinetic profiling to evaluate their complex stability with the receptor site by performing MD (molecular dynamic) simulation. GROMACS 2022. MD simulations of the selected ligand–*S. aureus* complexes were performed for 100 ns using two computational programs. The systems were equilibrated under low-temperature and constant pressure (NPT) conditions, with positional restraints followed by gradual temperature elevation to achieve a stable and balanced state. The 100 ns trajectories were analysed using energy, RMSD, RMSF, radius of gyration (Rg) and solvent-accessible surface area (SASA) parameters to assess the structural stability and dynamic behaviour of the complexes.

Density functional theory (DFT) analysis: The most active compounds (**A1** and **A9**) were examined for the DFT calculations using Schrödinger Suite2022 software, which is based on molecular docking and molecular simulation data. The B3LYP method was used to construct a 6-311+G(d,p) basis set. The HOMO and LUMO of both molecules were optimized to assess their electronic characteristics. The LUMO reflects electron-accepting ability, while the HOMO represents electron-donating tendency. Quantum mechanical descriptors including electron affinity (A), ionization potential (I), electronegativity (χ), chemical potential (μ) and hardness (η), were calculated to evaluate the electronic properties and chemical reactivity of the molecules. These descriptors were measured by applying the Koopman's theorem and Parr approximation eqns. 1-3 below:

$$\mu = \frac{(E_{HOMO} + E_{LUMO})}{2} \quad (1)$$

$$\eta = \frac{(E_{LUMO} - E_{HOMO})}{2} \quad (2)$$

$$\omega = \frac{\mu^2}{2\eta} \quad (3)$$

Molecular electrostatic potential (MEP) maps were used to identify the electrophilic and nucleophilic regions of the compounds. Electron-deficient regions (blue) represent potential sites for nucleophilic attack, whereas electron-rich regions (red) indicate favourable sites for electrophilic attack.

RESULTS AND DISCUSSION

A series of novel triazine–sulfonamide derivatives (**A1-A12**) was synthesized following the route outlined in **Scheme-I**. The synthesis involved sequential nucleophilic substitution reactions, with intermediate **3** serving as the key intermediate for the final coupling step in DMF to afford the target derivatives. All the synthesized compounds were characterized by IR, ^{1}H NMR and ^{13}C NMR spectroscopy. In the ^{1}H NMR spectra, the N–H proton attached to the triazine-linked cyclic

amine appeared as a broad singlet or in some cases, a broad doublet at δ 5.0-6.5 ppm (1H). The assignments were confirmed by D_2O exchange experiments, in which the corresponding resonances disappeared upon D_2O addition, confirming their exchangeable nature. The observed integration values were consistent with the proposed structures and accounted for all exchangeable and non-exchangeable protons.

Antimicrobial activity: The synthesized triazine–sulfonamide hybrids (**A1-A12**) showed variable antimicrobial activity against the tested microorganisms (Table-1). Compound **A1** showed the lowest MIC against *E. coli* (1.05 ± 0.06 μg/mL), while **A10** was most active against *S. aureus* (2.11 ± 0.08 μg/mL). Compounds **A4** and **A12** showed strong activity against *B. subtilis* (2.14 ± 0.08 μg/mL), *C. albicans* (1.11 ± 0.05 μg/mL) and P. aeruginosa (1.19 ± 0.05 μg/mL), respectively. A5 showed the best activity against *A. niger* (2.41 ± 0.09 μg/mL). Several active derivatives exhibited lower MIC values than ciprofloxacin against the corresponding bacterial strains.

Molecular docking: Molecular docking was performed to examine the binding of the synthesized compounds within the active site of dihydrofolate reductase (PDB ID: 1RX3), using ciprofloxacin and trimethoprim as reference drugs. The docking scores and key ligand–protein interactions are shown in Fig. 1. The docking results showed a general relationship between binding affinity and antimicrobial activity, with compounds **A1** and **A12** showing the closest agreement between computational and experimental results. Substituent variation on the terminal aromatic ring influenced both DHFR binding and antimicrobial activity. *para*-Electron-withdrawing groups, particularly those capable of polar or hydrogen-bonding interactions, were associated with favourable docking scores and antimicrobial activity. Nitrogen-containing heteroaromatic substituents likewise showed good activity in selected derivatives. These findings provide a preliminary structure–activity relationship in which the electronic and interaction properties of the terminal aromatic substituent appear to influence biological activity, although a definitive substituent-dependent SAR cannot be established from the present series.

Molecular dynamic simulation: To evaluate the thermodynamic stability of compounds **A1**, **A9**, **A10**, **A12** and the standard drug ciprofloxacin with the DHFR inhibitors, MD simulation was performed for a duration of up to 100 ns. The findings showed that every macromolecular complex could endure an MD simulation in GROMACS software version 2022 for 100 ns.2. To measure their thermodynamic stability, the macromolecular backbone's structure was modified and its RMSD was evaluated. The macromolecule complex comprising ligands **A1** and **A12** was found to include ten flexible bonds with thirty-four heavy atoms out of sixty-one atoms. The complex of ligand **A12** exhibited potent binding efficiency with receptor site having RMSD fluctuation ranging from 2.4-4.8 Å and ligand fluctuated between 7-10 Å. Apo-protein, query ligands and positive control have been compared using the GROMACS metrics RMSD, energy, radius of gyration, RMSF, SASA and MMPBSA, as shown in Table-2.

The RMSD and RG plots for complexes **A1**, **A12** and the standard drug (Fig. 2) indicate relatively stable trajectories, although **A1** shows comparatively higher structural deviation than **A12** and the standard drug. Fig. 3 further supports these observations through the radius of gyration and SASA profiles, which suggest differences in the molecular compactness and solvent exposure while maintaining the stable behaviour throughout the simulation.

DFT studies: DFT calculations were performed for representative compounds **A1** and **A9** (Fig. 4), selected based on their favourable structural and energetic stability. The analysis was used to examine the electronic structure, molecular stability and reactivity of these compounds rather than to establish a direct relationship between DFT parameters and antimicrobial or docking activity. Both compounds showed well-defined HOMO and LUMO distributions across the molecular framework. The HOMO–LUMO energy gap (ΔE) and quantum molecular descriptors including hardness (η), electron affinity (A), electronegativity (χ), ionization potential (I), electrophilicity index (ω) and chemical potential (μ), were calculated using Koopmans' theorem. These parameters provided insight into the electronic stability and chemical reactivity of **A1** and **A9**.

Conclusion

A novel series of sulfonamide-linked 1,3,5-triazine hybrids (**A1-A12**) was synthesized and evaluated for antimicrobial activity using DHFR docking (PDB ID: 1RX3) and *in vitro* assays. Compound **A1** showed the strongest DHFR binding

TABLE-1
ANTIMICROBIAL ACTIVITY DATA OF NEWLY SYNTHESIZED TRIAZINE-SULFONAMIDE DERIVATIVES (**A1-A12**)

Compd.	*S. aureus*	*B. subtilis*	*E. coli*	*P. aeruginosa*	*A. niger*	*C. albicans*
A1	3.21 ± 0.12	2.84 ± 0.10	1.05 ± 0.06	2.31 ± 0.09	2.23 ± 0.08	2.10 ± 0.07
A2	2.16 ± 0.08	2.44 ± 0.09	3.33 ± 0.11	–	–	–
A3	4.18 ± 0.15	3.19 ± 0.12	5.14 ± 0.18	2.22 ± 0.09	10.00 ± 0.25	6.10 ± 0.20
A4	3.36 ± 0.11	2.14 ± 0.08	1.12 ± 0.05	3.35 ± 0.12	3.25 ± 0.11	1.11 ± 0.05
A5	9.11 ± 0.22	4.56 ± 0.16	3.20 ± 0.12	7.23 ± 0.21	2.41 ± 0.09	–
A6	3.30 ± 0.11	2.77 ± 0.10	–	3.68 ± 0.13	4.44 ± 0.15	3.48 ± 0.12
A7	3.66 ± 0.12	–	2.64 ± 0.09	–	2.65 ± 0.09	3.26 ± 0.11
A8	2.12 ± 0.08	2.65 ± 0.09	3.55 ± 0.12	1.94 ± 0.07	3.31 ± 0.11	4.10 ± 0.14
A9	4.01 ± 0.14	5.23 ± 0.18	6.18 ± 0.20	2.55 ± 0.09	–	3.26 ± 0.11
A10	2.11 ± 0.08	2.21 ± 0.08	–	3.68 ± 0.13	6.99 ± 0.21	1.12 ± 0.05
A11	4.05 ± 0.14	–	1.23 ± 0.06	2.55 ± 0.09	–	5.10 ± 0.17
A12	–	2.99 ± 0.10	–	1.19 ± 0.05	3.22 ± 0.11	–
Ciprofloxacin	11.10 ± 0.28	15.10 ± 0.35	14.00 ± 0.32	12.10 ± 0.30	–	–

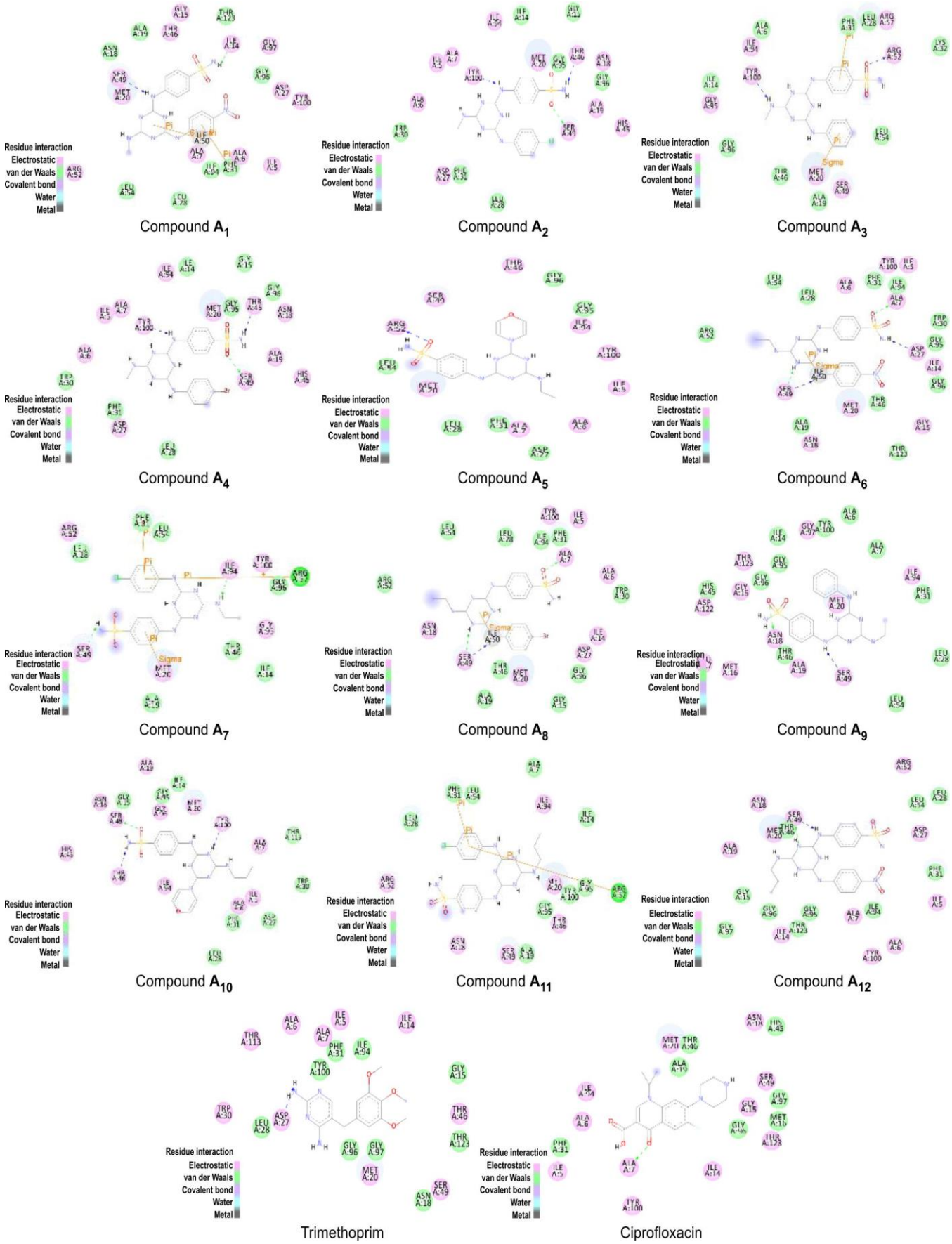

Fig. 1. Docking score and key interaction of compounds (**A1-A12**) against DHFR

TABLE-2
COMPARISON OF DHFR APO-PROTEIN AND DHFR COMPLEXES WITH LIGANDS (A_1, A_{12} AND CIPROFLOXACIN)

		dhfr_1rx3_prot-rmsd_mdsim.xvg	dhfr_Complex_A_1-rmsd_mdsim.xvg	dhfr_Complex_A_{12}-rmsd_mdsim.xvg	dhfr_Complex_Cipro-rmsd_mdsim.xvg
RMSD	Mean	0.220	0.129	0.159	0.118
	Std.	0.069	0.029	0.036	0.018
Energy	Mean	-275857.430	-270403.091	-270460.521	-268290.159
	Std.	830.908	824.606	838.803	830.779
Radius of gyration	Mean	1.558	1.569	1.574	1.567
	Std.	0.010	0.009	0.012	0.007
RMSF	Mean	0.164	0.128	0.145	0.113
	Std.	0.076	0.055	0.069	0.052
SASA	Mean	90.585	91.590	92.739	91.413
	Std.	2.148	1.572	1.798	1.453
MMPBSA	Mean	-32.956	-36.335	-35.000	
	Std.	7.525	5.109	3.800	

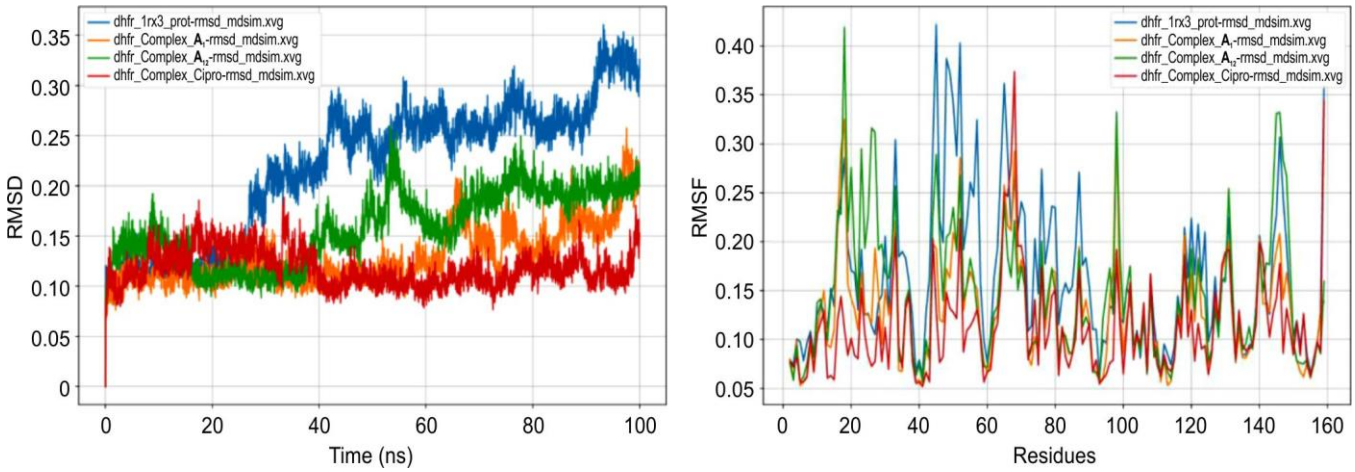

Fig. 2. Comparison of RMSD & RMSF of complex over 100 ns A_1, A_{12} and ciprofloxacin

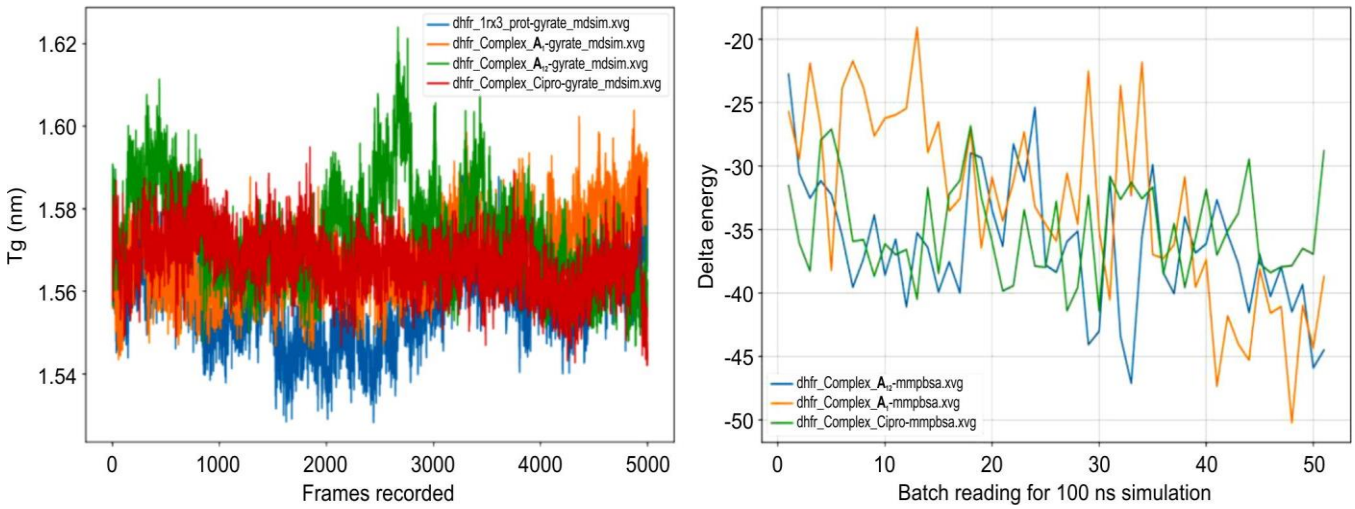

Fig. 3. Comparison of radius of gyration & MMPBSA of complex A_1, A_{12} and ciprofloxacin

(-10.2 kcal/mol) and the lowest MIC against *E. coli* (1.05 ± 0.06 μg/mL), compared with ciprofloxacin (-9.1 kcal/mol; 14.00 ± 0.32 μg/mL) and trimethoprim (-7.6 kcal/mol). Compounds A_4, A_{10} and A_{12} likewise showed favourable antimicrobial profiles, supported by hydrogen-bonding, π-π stacking and halogen-bonding interactions. *para*-Electron-withdrawing groups and nitrogen-containing heteroaromatic rings were associated with favourable DHFR binding and antimicrobial activity. The combined computational and experimental findings support the sulfonamide-linked 1,3,5-triazine scaffold as a useful platform for further antimicrobial development.

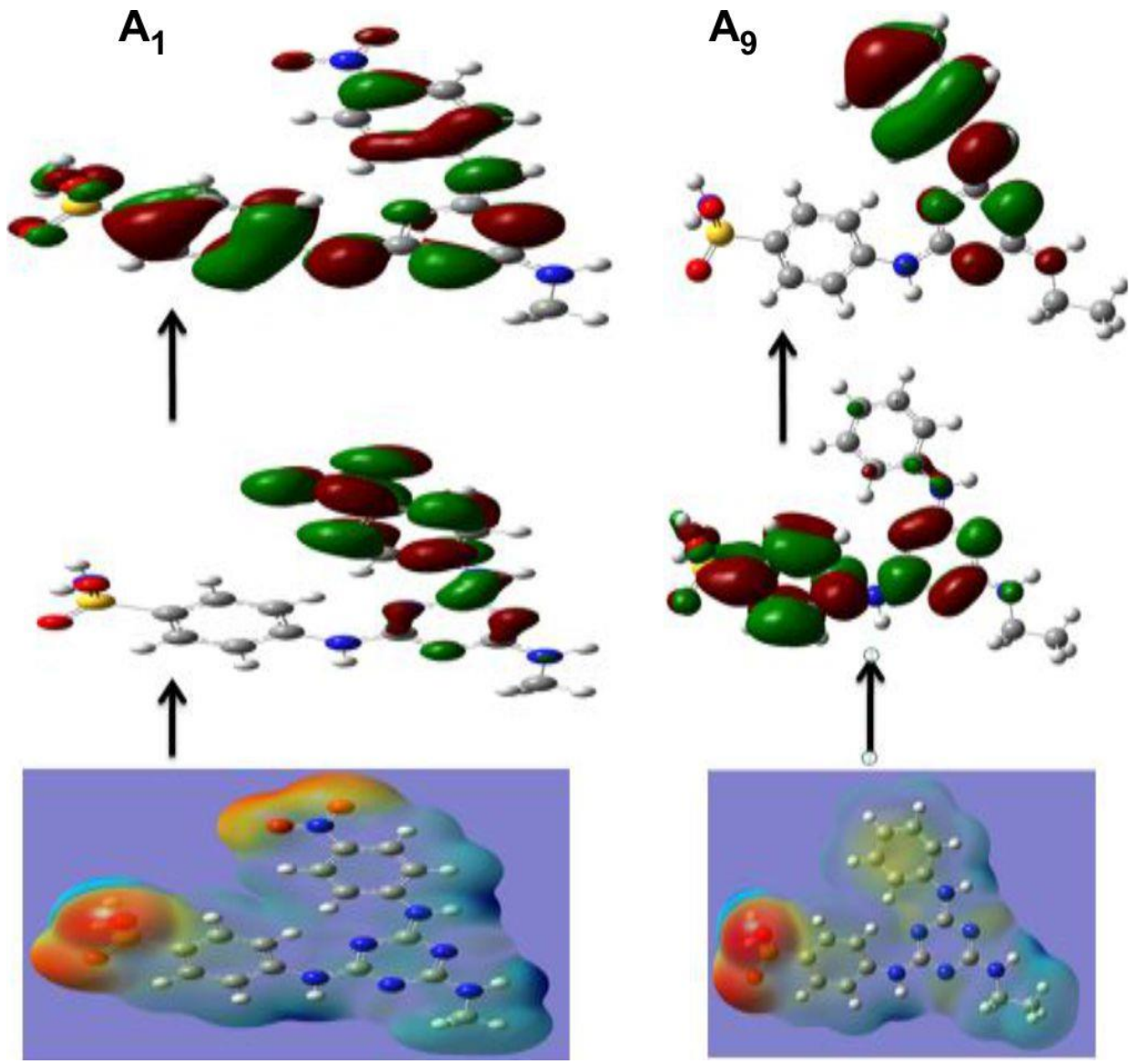

Fig. 4. HOMO, LUMO and MEP analysis of compound **A1**, **A9** through DFT

ACKNOWLEDGEMENTS

The authors are highly thankful to School of Healthcare and Allied Sciences, GD Goenka University, Sohna, for providing the support that facilitated the study.

CONFLICT OF INTEREST

The authors declare that there is no conflict of interests regarding the publication of this article.

DECLARATION OF AI-ASSISTED TECHNOLOGIES

During the preparation of this manuscript, the authors used an AI-assisted tool(s) to improve the language and no data, results or scientific conclusions were generated by AI. All analyses, interpretations and conclusions are the authors' own. The authors reviewed and edited the content and take full responsibility for the published work.

REFERENCES

1. A. Szymanowska, D. Radomska, R. Czarnomysy, M. Mojzych, K. Kotwica-Mojzych, K.A. Bielawski and A. Bielawska, *J. Enzyme Inhib. Med. Chem.*, **39**, 2343352 (2024); https://doi.org/10.1080/14756366.2024.2343352
2. M.M. Zafer, G.A. Mohamed, S.R. Ibrahim, S. Ghosh, C. Bornman and M.A. Elfaky, *Arch. Microbiol.*, **206**, 101 (2024); https://doi.org/10.1007/s00203-023-03826-z
3. M. Sanduja, J. Gupta, R. Rawat, U. Singh and S.M. Verma, *J. Appl. Pharm. Sci.*, **10**, 1 (2020); https://doi.org/10.7324/JAPS.2020.103001
4. A.C. Lele, A. Raju, M.P. Khambete, M.K. Ray, M.G.R. Rajan, M.A. Arkile, N J. Jadhav, D. Sarkar and M.S. Degani, *ACS Med. Chem. Lett.*, **6**, 1140 (2015); https://doi.org/10.1021/acsmedchemlett.5b00367
5. I. Pathan, A. Raza, A. Sahu, M. Joshi, Y. Sahu, Y. Patil, M.A. Raza and Ajazuddin, *Med. Drug Discov.*, **28**, 100223 (2025); https://doi.org/10.1016/j.medidd.2025.100223
6. N.P. Dalbanjan and S.K. Praveen, *Indian J. Microbiol.*, **64**, 879 (2024); https://doi.org/10.1007/s12088-024-01355-x

7. A.A. Aslam, M. Ahmed, M.H.A. Mughram, M.H.-U.-R. Mahmood, S. Basheer, R. Hussain, E. Eiman, M. Sanaullah, H. Raza, A. Saeed, M. Hassan and D.N. Iqbal, *Chem. Biodivers.*, **22**, e202403434 (2025); https://doi.org/10.1002/cbdv.202403434
8. B.I. Schweitzer, A.P. Dicker and J.R. Bertino, *FASEB J.*, **4**, 2441 (1990); https://doi.org/10.1096/fasebj.4.8.2185970
9. R. Sehrawat, P. Rathee, S. Khatkar, E. Akkol, M. Khayatkashani, S.M. Nabavi and A. Khatkar, *Curr. Med. Chem.*, **31**, 799 (2024); https://doi.org/10.2174/0929867330666230310091510
10. H. Azevedo-Barbosa, D.F. Dias, L.L. Franco, J.A. Hawkes and D.T. Carvalho, *Curr. Med. Chem.*, **20**, 2052 (2020); https://doi.org/10.2174/1389557520666200905125738
11. J.R. Schnell, P.E. Dyson, *Annu. Rev. Biophys. Biomol. Struct.*, **33**, 119 (2004); https://doi.org/10.1146/annurev.biophys.33.110502.133613
12. A. Wróbel and D. Drozdowska, *Curr. Med. Chem.*, **28**, 910 (2021); https://doi.org/10.2174/0929867326666191016151018
13. S.A. Adcock and J.A. McCammon, *Chem. Rev.*, **106**, 1589 (2006); https://doi.org/10.1021/cr040426m
14. S.K. Verma, R. Verma, F. Xue, P.K. Thakur, Y.R. Girish and K.P. Rakesh, *Bioorg. Chem.*, **105**, 104400 (2020); https://doi.org/10.1016/j.bioorg.2020.104400
15. T. Brinck and J.H. Stenlid, *Adv. Theory Simul.*, **2**, 1800149 (2019); https://doi.org/10.1002/adts.201800149
16. E.M. Hussein, M.M. Al-Rooqi, S.M. Abd El-Galil and S.A. Ahmed, *BMC Chem.*, **13**, 91 (2019); https://doi.org/10.1186/s13065-019-0603-x
17. S. Shahzad, M. A. Qadir, M. Ahmed, S. Ahmad, M.J. Khan, A. Gulzar, and M. Muddassar, *RSC Adv.*, **10**, 42983 (2020); https://doi.org/10.1039/D0RA09051D
18. R. Sehrawat, P. Rathee, E.K. Akkol, M. Khayatkashani, S. Khatkar, S.M. Nabavi and A. Khatkar, *Curr. Med. Chem.*, **31**, 799 (2024); https://doi.org/10.2174/0929867330666230310091510
19. S. Hawser, S. Lociuro and K. Islam, *Biochem. Pharmacol.*, **71**, 941 (2006); https://doi.org/10.1016/j.bcp.2005.10.052
20. R.A. Azzam, R.E. Elsayed and G.H. Elgemeie, *ACS Omega*, **5**, 10401 (2020); https://doi.org/10.1021/acsomega.0c00280
21. C.R. Bourne, *Antibiotics*, 3, 1 (2014); https://doi.org/10.3390/antibiotics3010001
22. S. Babalola, N. Igie and I. Odeyemi, *Pharm. Fronts*, **4**, e250 (2022); https://doi.org/10.1055/s-0042-1759688
23. O. Trott and A.J. Olson, *J. Comput. Chem.*, **31**, 455 (2010); https://doi.org/10.1002/jcc.21334
24. M.R. Sawaya and J. Kraut, *Biochemistry*, **36**, 586 (1997); https://doi.org/10.1021/bi962337c
25. S.M. Reeve, D. Si, J. Krucinska, Y. Yan, K. Viswanathan, S. Wang, G.T. Holt, M.S. Frenkel, A.A. Ojewole, A. Estrada, S.S. Agabiti, J.B. Alverson, N.D. Gibson, N.D. Priestly, A.J. Wiemer, B.R. Donald and D.L. Wright, *ACS Infect. Dis.*, **5**, 1896 (2019); https://doi.org/10.1021/acsinfecdis.9b00222
26. M.A. Rauf, S. Zubair and A. Azhar, *Int. J. Basic Appl. Sci.*, **4**, 168 (2015); https://doi.org/10.14419/ijbas.v4i2.4123
27. S.A. Hollingsworth and R.O. Dror, *Neuron*, **99**, 1129 (2018); https://doi.org/10.1016/j.neuron.2018.08.011
28. M. Hudek, University Of Strathclyde. *Chemical and Process Engineering*. (2024); https://doi.org/10.48730/3hgr-9578
29. N.R. Stanley, F. Sargent, G. Buchanan, J. Shi, V. Stewart, T. Palmer and B.C. Berks, *Mol. Microbiol.*, **43**, 1005 (2002); https://doi.org/10.1046/j.1365-2958.2002.02797.x